Clays and Clay Minerals, Vol. 53, No. 3, 250–267, 2005.

CLAY MINERALOGY AND CHEMICAL COMPOSITION OF BENTONITES FROM THE GOUROUGOU VOLCANIC MASSIF (NORTHEAST MOROCCO)

MOHAMED DDANI[1,2], ALAIN MEUNIER[1,*], MOHAMED ZAHRAOUI[2], DANIEL BEAUFORT[1], MOHAMED EL WARTITI[2], CLAUDE FONTAINE[1], BOUBKER BOUKILI[2] AND BENACER EL MAHI[2]

[1] HYDRASA-UMR 6532 CNRS, Université de Poitiers, 40, avenue de Recteur Pineau, 86022 Poitiers, France
[2] Laboratoire de Géologie appliquée, Université Mohammed V, Faculté des Sciences Agdal, Département de Sciences de la Terre, avenue Ibn Batouta, BP 1014, Rabat, Morocco

Abstract—The Gourougou volcanic massif (northeastern Morocco) is actively prospected for bentonite deposits. Five bentonites originating from different environments were selected for the present study: hydrothermal alteration of obsidian perlite glass inside the volcanoes themselves (Providencia and Tribia deposits); alteration of pyroclastic flows in a marine shallow water to lagoonal lacustrine environment (Ibourhardayn deposit); ash falls in marine or lacustrine systems (Moulay Rachid and Melg el Ouidan (formerly Camp Berteau) deposits). All of these bentonites were probably formed from volcanic glass originating from a rhyolitic magma at different stages of differentiation as shown by slight variations of *REE* and incompatible element abundances. The crystal-chemical characteristics of the smectite vary according to alteration conditions: beidellite predominates in hydrothermal systems, whereas montmorillonite predominates in lagoonal and lacustrine environments, and mixed-layer beidellite-montmorillonite in the sea-water-altered pyroclastic flows. All these dioctahedral smectites exhibit a heterogeneous distribution of charge as shown by the presence of partially expandable (1 EG) or non-expandable (0 EG) layers in the K-saturation state. The proportion of the collapsed or partially expandable layers is not related to the average layer charge or to the cation exchange capacity. This militates for an overall heterogeneous charge distribution. Compared to other natural or experimental alteration systems of similar rhyolitic glass, the formation of beidellite or montmorillonite appears to be controlled by the amounts of Mg in the system.

Key Words—Alteration, CEC, Layer Charge, Smectite, Volcanic Glass.

INTRODUCTION

Bentonites are essentially composed of dioctahedral smectites, the crystallochemical composition of which occurs in the range of the montmorillonite–beidellite series (Boles and Surdam, 1979; Zielinski, 1982; Senkayi *et al*., 1984; Christidis and Dunham, 1993, 1997; Yamada *et al*., 1999; Huertas *et al*., 2000; Fiore *et al*., 2001). Many of the bentonites form through alteration of glassy ash and pyroclastic flows and are genetically related to explosive volcanism (Grim and Güven, 1978). Bentonite deposits may cover large areas and hence constitute efficient chrono-stratigraphical markers in sedimentary sequences (Huff *et al*., 1991). Because of industrial use, the term bentonite was also extended to massive clay deposits formed by hydrothermal alteration of the volcanic domes and their proximal pyroclastic glassy material (Linares, 1985).

It is well known that volcanic glass is highly reactive in the presence of water particularly when its interaction surface is increased by the volcanic processes (ashes or pumice). According to the pH and alkali concentration of the altering solutions, different secondary products are formed during the conversion such as zeolites and silica polymorphs. Despite significant progress due to experimental conversion of volcanic glass to smectite (Zielinski, 1979; De la Fuente, 2000 among others), the detailed mechanisms and rate-controlling factors for bentonite formation in natural environments are not fully understood. For example, transformation of glassy sediments to bentonite can be quick, *i.e.* a few hours or days (Berry, 1999) to a few years (Davies *et al*., 1979; Zielinski, 1980), or glassy volcanic material can persist for several hundreds of thousands to several million years (Keller *et al*., 1978; Imbert and Desprairies, 1987; Weaver, 1989; Hein and Scholl, 1978). When volcanic glass is altered to smectite, the crystal structure of the smectite by-product varies according to different parameters such as the composition of the parent rock or the physico-chemical characteristics of the geological environment (Christidis, 1998).

In many cases, the bentonite deposits which are unequivocally related to a parent rock and an alteration system are formed by hydrothermal alteration proximal to a volcanic center. However, bentonites of large areal extent form by alteration of more distal lava flows, air fall ashes under low-temperature conditions in the presence of sea water or meteoric water. Examination of different styles of alteration of volcanic glass to bentonite requires investigations at a regional scale that

* E-mail address of corresponding author:
alain.meunier@hydrasa.univ-poitiers.fr
DOI: 10.1346/CCMN.2005.0530305

include the source-rock volcanic domes and their associated altered pyroclastic flows or ash fall deposits at different distances from the volcanic center. This is the topic of the present study.

The paper provides new crystal-chemical data on dioctahedral smectites formed in bentonite deposits associated with the Gourougou volcanic massif (north-eastern Morocco). This region offers the opportunity to investigate several different types of bentonite deposits formed from the same or a very similar volcanic source. The studied deposits are representative of the principal types of geological environments expected for the formation of bentonites: hydrothermal alteration of glassy material close to the volcanic domes and alteration of surrounding volcano-sedimentary deposits in various depositional environments (marine, lagoonal or fluvio-lacustrine) at a regional scale.

GEOLOGICAL SETTING

Subduction in the Alboran region closed marine gateways between the Atlantic Ocean and Mediterranean Sea (Duggen *et al*., 2004) inducing orogenesis and associated volcanism. The Rif mountains in northeast Morocco belong to the circum-Mediterranean Alpine orogenesis. During their tectonic history, several sedimentary basins have been formed during the Tortonian-Messinian ages and the Pliocene epoch (Pique *et al*., 1998). At the same time as the subduction processes, intense volcanic activity formed the Gourougou complex (Maury *et al*., 2000). The structure of this massif (Figure 1a) indicates that the first step was sub-marine, explosive volcanic activity. Then the activity became progressively aerial and effusive (Hernandez, 1983; El Bakkali, 1995). During the Messinian age, the south-eastern part of Spain and northern Morocco and Algeria formed a patchwork of basins separated by islands in which lavas, pyroclastic flows and ashes were deposited (Benson *et al*., 1991). These basins isolated several types of coastal environments: marine, lagoonal or fluvio-lacustrine. In various locations, the pyroclastic flows and ashes have been transformed into bentonite deposits.

According to their geological relationships with the volcanoes and the sedimentary environments, three types of bentonite deposits have been distinguished.

Bentonites formed by hydrothermal alteration of the lava domes

Several quarries have been opened in altered perlites, breccia or pyroclastic flows. Two were sampled at Providencia and Tribia (Tidiennit volcano): (1) Providencia bentonite, In-Haddou or Amar, eastern flank of the Tidiennit massif (Figure 1b). The sub-aquatic volcanic activity produced perlites which were strongly brecciated. The pyroclastic flows (TB) were deposited by aerial volcanic activity. Perlites (Pr) were intruded later by a massive rhyolite body (Rh) around which hydrothermal activity has severely argillized the porous breccia (Bn). Close to the perlite contact, the pyroclastic flows have been cemented by silica deposits (cristobalite) of 0.5–1 m thick (TS). An alteration profile has been sampled from the non-argillized perlite (reference sample) to a completely argillized porous rock. The rhyolite was sampled for comparison with the perlite. (2) Tribia bentonite, northwest flank of the Tidiennit massif (Figure 1c). The perlite (Pr) and rhyolite (Rh) bodies are adjacent to a N45 normal fault and overlain by pyroclastic flows (TB) and ash deposits (VA). The brecciated zone is argillized in a 15 m thick zone along the fault (Bn). The alteration intensity decreases with increasing distance from the rhyolite body. Cristobalite is observed locally in the altered zone.

Bentonites replacing pyroclastic flows in the vicinity of the volcanoes (Ibourhardayn, 5 km south of Tidiennit massif)

Bentonites form regular beds which are several meters thick. They originated from the argillization of volcanic ash deposits and brecciated pyroclastic flows (AB and ATB) which exhibit typical transport features. Both are intercalated with limestone beds (Ll) and cinerite beds (Cn) in the upper part of the deposit (Figure 1d). They overly a sandy marl basement with bio-detrital levels containing algae and bryozoa. The flora and fauna are typical of marine shallow water to lagoonal-lacustrine environments (Ait Brahim, 1991).

Bentonite beds, a few tens of centimeters thick, intercalated into sedimentary formations at several tens of kilometers from the volcanoes

The ashes have been transported air-borne over tens of kilometers from the volcanic centers.

Moulay Rachid bentonite; 30 km southeast of the Tidiennit massif (Figure 1e). The bentonite (Bn) forms a 20–25 cm thick bed at the base of a cinerite deposit (Cn). It is overlain by a sand or polygenic conglomerate (S) which is the lowest formation of the regional Messinian series. The fauna comprises marine lamellibranchiata, brachiopods and gastropods.

Melg el Ouidan bentonite (formerly Camp Berteau); 80 km south southeast of Tidiennit massif (Figure 1f). Two thin bentonite beds (5–10 cm thick) are intercalated in a lagoonal-lacustrine sedimentary series dominated by gypsum-bearing marls and limestones (Ll). The two bentonite beds (Bn) are separated by a blue soapy calcareous clay (BSC). This sedimentary series is overlain by rhyolitic cinerites (Cn) which are considered to have a similar origin to the parent ash of the bentonite. The cinerites have no genetic link with the Messinian Guiliz volcano which is close to the deposit. They are related to the Gourougou volcanic massif (Hernandez, 1986).

https://doi.org/10.1346/CCMN.2005.0530305 Published online by Cambridge University Press

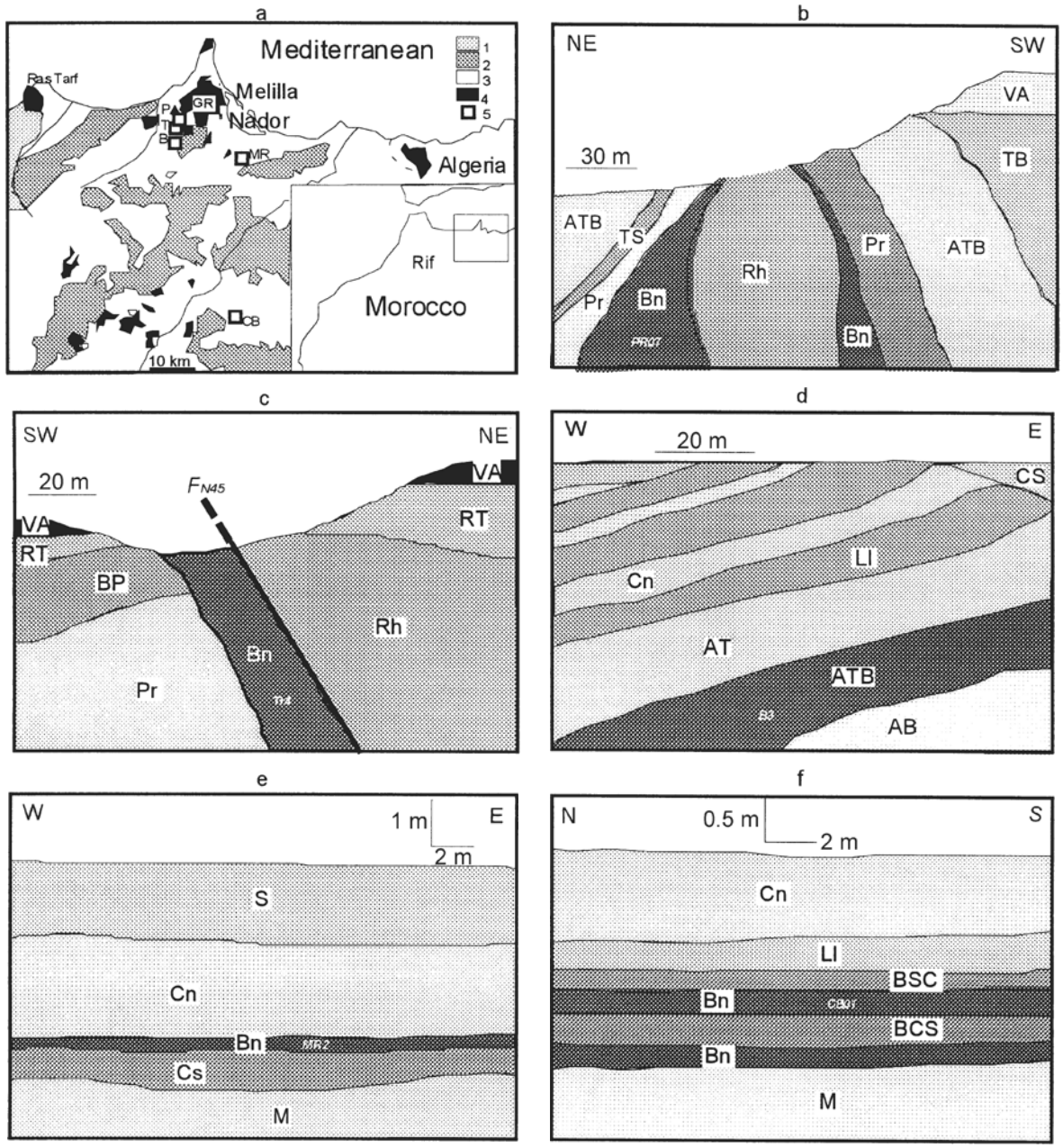

Figure 1. The Gourougou volcanic area (northern Morocco). (a) Simplified geological map. P, T, B, MR, CB indicate the locations of the Providencia, Tribia, Ibourhardayn, Moulay Rachid and Melg el Ouidan (formerly Camp Berteau) bentonite deposits, respectively. GR: Gourougou massif, (1) Mésorif (nappes); (2) folded Jurassic and Cretaceous fore-land formations; (3) Neogene unfolded sediments; (4) volcanic formations; (5) studied bentonite deposits. (b) Providencia hydrothermal system. (c) Tribia hydrothermal system. (d) Ibourhardayn pyroclastic flow deposit. (e) Moulay Rachid ash deposit. MR2. (f) Melg el Ouidan (formerly Camp Berteau) ash deposit. The locations of the samples selected for the study (PR07, Tr4, B3, MR2, CB01) are indicated for each outcrop. AB: altered breccia, ATB: altered pyroclastic flow and breccia, AT: altered pyroclastic flow, Bn: bentonite, BP: brecciated perlite, BSC: blue soapy calcareous clay, Cn: cinerite, CS: coarse sandstone, F_{N45}: N45 normal fault, Ll: lacustrine limestone, M: marl, Pr: Perlite, Rh: rhyolite, RT: rhyolite pyroclastic flow, S: sandstone, TB: unaltered pyroclastic flow and breccia, TS: silicified pyroclastic flow, VA: volcanic ash.

METHODS AND ANALYTICAL TECHNIQUES

The sample richest in clay was selected from each of the five bentonite deposits to be studied in detail (Table 1). Polished thin-sections were made after resin induration of the argillized samples. Freshly fractured rock fragments were observed using a JEOL JSM6400 scanning electron microscope (SEM) equipped with an energy dispersive spectrometer (EDS). The bentonite

https://doi.org/10.1346/CCMN.2005.0530305 Published online by Cambridge University Press

Table 1. Sampling and environment of formation of bentonite deposits.

Bentonite deposit	Sample name	Types of alteration	Types of geological setting
Providencia	PR07	Hydrothermal alteration of the lava domes (open system)	Lava and breccia perlite
Tribia	Tr4	Hydrothermal alteration of the lava domes (open system)	Breccia perlite
Ibourhardayn	B3	Alteration in lagoonal-lacustrine environments (closed system)	Pyroclastic flow and pyroclastics intercalated within limestone beds. Algae and bryozoa are typical of lagoonal-lacustrine environments
Moulay Rachid	MR2	Alteration in marine environment (closed system)	Volcanic ash deposit. The fauna comprises marine lamellibranchiata, brachiopods and gastropods
Melg el Ouidan	CB01	Alteration in lagoonal-lacustrine environment (closed system)	Volcanic ash intercalated in a lagoonal-lacustrine sedimentary series dominated by gypsum-bearing marls and limestones

samples were gently ground after drying at 60ºC and the powders dispersed ultrasonically into distilled water. The <2 μm fraction was separated using centrifugation and Ca-, Na- and K-saturated by dispersion and stirring for 3 h in 1 N $CaCl_2$, NaCl or KCl solutions, respectively. The excess chloride was rinsed out using ethyl alcohol until no white precipitate was formed with $AgNO_3$. Part of the K-saturated samples was Ca exchanged afterwards using a 1 N $CaCl_2$ solution (K-Ca samples). In addition, the octahedral charge of each Ca-saturated sample was neutralized using the Hofmann and Klemen (1950) treatment: Li saturation and heating at 300ºC for 12 h.

Several oriented mounts were prepared for each sample after Ca, K, K-Ca saturations and ethylene glycol solvation in order to study the variations of the swelling properties related to the layer-charge distribution heterogeneity in the smectite layers (Calarge *et al*., 2003). Randomly oriented powders were prepared from the untreated samples. X-ray diffraction (XRD) patterns were recorded using a Siemens D500 diffractometer (CuKα radiation, 40 kV and 40 mA), equipped with a stepping motor drive on the goniometer (SOCABIM DACO system) and a Kevex PSI detector (resolution: 260 eV). The angular range, scanning step size and counting time analytical conditions were 2–20 and 3–65º2θ, 0.025 and 0.040º2θ, 4 s and 6 s for oriented preparations and randomly oriented powders, respectively. Specific XRD patterns from randomly oriented powders using a greater counting time (8 s) were obtained in the 33–41 and 58–64º2θ angular ranges for a detailed study of the 20, 13 and 060 reflections which are typical of the layer stacking structure and octahedral occupancy of phyllosilicates, respectively.

The decomposition of the XRD patterns was conducted according to the recommendations of Lanson (1997): the background was assumed to be linear whenever possible (2θ ⩾ ~8º), and interpolated assuming a Lorentz factor-like shape in low-angle regions for which the interpolation domain is very large; a satisfactory fit to the experimental data was obtained using a minimum number of elementary Gaussian or Lorentzian curves.

Each elementary reflection (Gaussian or Lorentzian) is characterized by three parameters: position, intensity and full width at half maximum intensity (FWHM). Narrow (FWHM <1) and broad (FWHM >1) reflections in the 8–11º2θ CuKα angular range are related to two- and three-component mixed-layer minerals, respectively (Meunier *et al*., 2004). The saddle/peak ratio in the low-angle region was measured using XRD patterns of oriented preparations of Ca-saturated samples in the ethylene glycol-solvated state (Inoue *et al*., 1989).

Major and minor elements including rare earth elements (*REE*) were analyzed from bulk rocks using inductively coupled plasma-emission spectroscopy (ICP-ES) at the Centre de Recherche Pétrographique et Géochimique (CRPG) in Vandœuvre-lès-Nancy (France). Trace elements were analyzed using inductively coupled plasma-mass spectroscopy (ICP-MS). The cation exchange capacity (CEC) of the <2 μm fraction was obtained from NH_4^+-exchanged Ca, K and (K-Ca)-saturated samples. The excess NH_4^+ was carefully washed out with ethanol. The CEC linked to the tetrahedral charge was obtained from Li-300ºC samples which had been saturated with Mg^{2+} cations, the excess Mg^{2+} ions being carefully washed out with ethanol. Then Mg^{2+} was exchanged by NH_4^+ and the Mg^{2+} cations in the solution were analyzed using atomic absorption spectrophotometry.

The primary and secondary minerals and the glass relics have been analyzed in thin-sections using a CAMECA SX50 electron microprobe equipped with

https://doi.org/10.1346/CCMN.2005.0530305 Published online by Cambridge University Press

wavelength-dispersive spectrometers. The analyzed elements were Na, Mg, Al, Si, K, Ca, Mn and Fe (Ti is considered to be incorporated in separate oxide phases). The microprobe was calibrated using synthetic and natural standards ($MnTiO_3$, hematite, albite, orthoclase and diopside). Corrections were performed using a ZAF program. The analytical conditions were 4 nA, 15 kV, 2–4 μm, 10 s for current intensity, accelerating voltage,

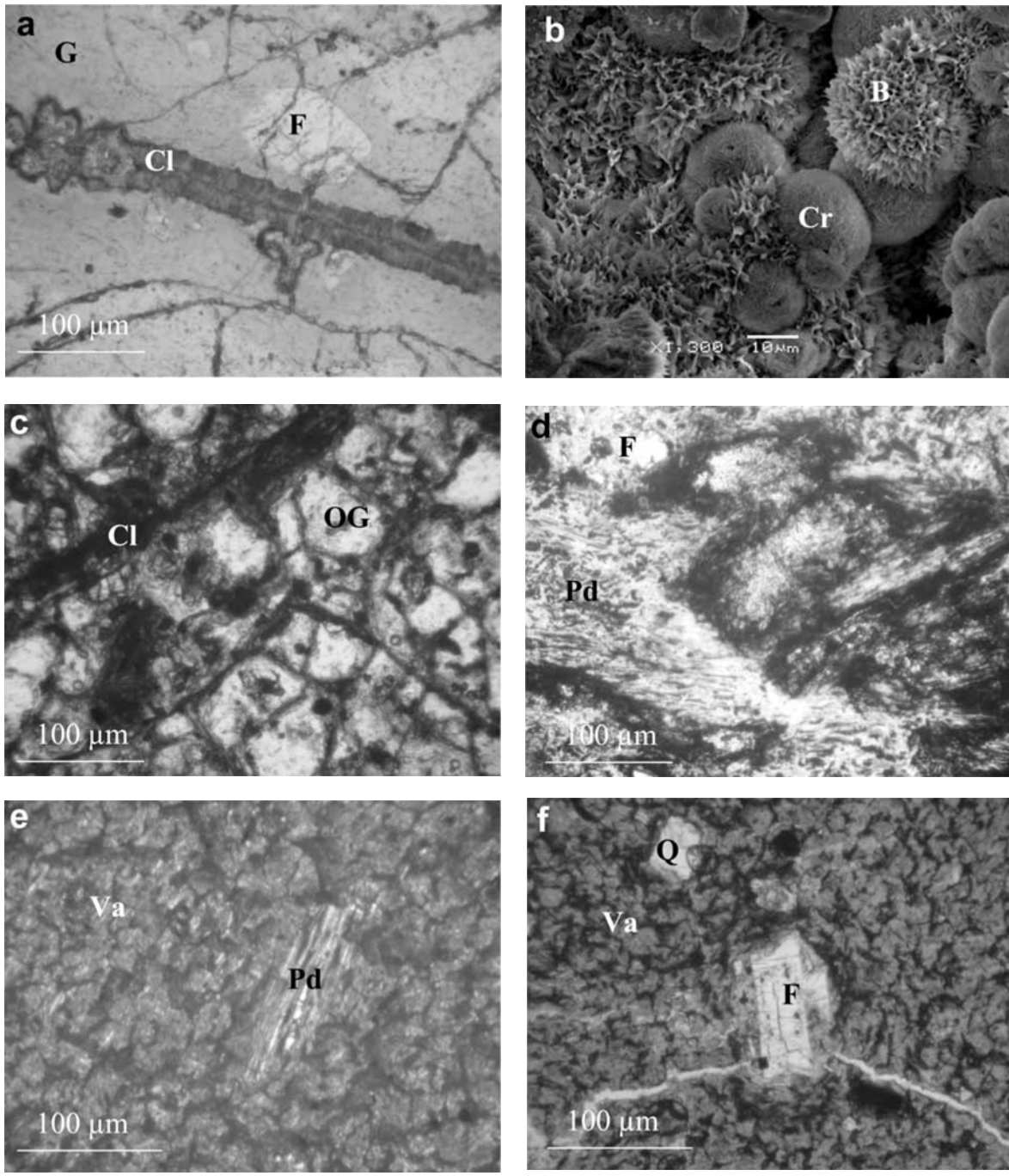

Figure 2. Optical and SEM images of the microstructure of bentonites. (a) Hydrothermal alteration of obsidian glass along perlitic curved fractures (Providencia). (b) Honeycomb microstructures of beidellite with cristobalite spherolites forming the wallrock deposit in a fracture in the perlitic glass (Providencia). (c) Pervasive alteration around perlitic fractures (Tribia). (d) Alteration of pumice debris in a pyroclastic flow breccia (Ibourhardayn). (e) Alteration of coarse volcanic ash deposit containing pumice debris (Moulay Rachid). (f) Alteration of fine-grained volcanic ash deposit containing small phenocrysts of K-feldspar and quartz at Melg el Ouidan (formerly Camp Berteau). B: beidellite, Cl: clays, Cr: cristobalite, F: feldspar, G: glass, OG: obsidian glass, Pd: pumice debris, Q: quartz, Va: volcanic ash.

https://doi.org/10.1346/CCMN.2005.0530305 Published online by Cambridge University Press

spot size and counting time per element, respectively. The relative error for each analyzed element is <1.5% of its oxide wt.%.

RESULTS

Petrography and mineralogy of bentonites and altered rocks

The perlitic lavas in Providencia and Tribia volcanoes were strongly altered through a dense fracture network (Figure 2a). The argillized zones (PR07 and Tr4 samples) are highly porous and composed of clay material exhibiting a honeycomb texture and cristobalite spherules (Figure 2b). The alteration propagates from the fractures into the massive glass until replacement is complete (Figure 2c). Similar alteration features are observed in the breccia fragments in the lower pyroclastic flow at Ibourhardayn (sample B3). These fragments are embedded inside a pumice-rich matrix which is massively altered. Pumice predominates in the upper pyroclastic flow level. In spite of an intense argillization, the structure of the pumice elements is preserved (Figure 2d). The shape of ash grains is conserved in the Moulay Rachid and Melg el Ouidan bentonite deposits. The mean sizes of the ash grains for the MR2 and CB01 samples are 90 and 40 μm, respectively (Figure 2e–f). In both cases, pumice structure and crystal debris were preserved but all the glass has been argillized.

The mineralogical investigation based on SEM observations and XRD patterns of randomly oriented samples (Figure 3a) shows that the samples comprise minor amounts of primary igneous minerals (plagioclase, K-feldspar, biotite, quartz and apatite) embedded in a matrix essentially consisting of smectite ± kaolinite. Locally, cristobalite, Fe oxide and calcite are present as minor alteration products.

The smectite is characterized by an intense broad d_{001} peak in the low-angle region. The d_{001} spacing varies from 13 to 15 Å according to the dominant interlayer cation: Ca^{2+} for CB01, Na^{+} for MR2 and B3. The other samples are characterized by intermediate positions. Both exhibit a broad asymmetric 20,13 peak. The absence of any modulation (Figure 3b) indicates that in all samples the stacking of the smectite layers is turbostratic (Reynolds, 1992). The position of the d_{060} peak varies from 1.496 to 1.500 Å in all the samples indicating that all smectites are dioctahedral (Figure 3c).

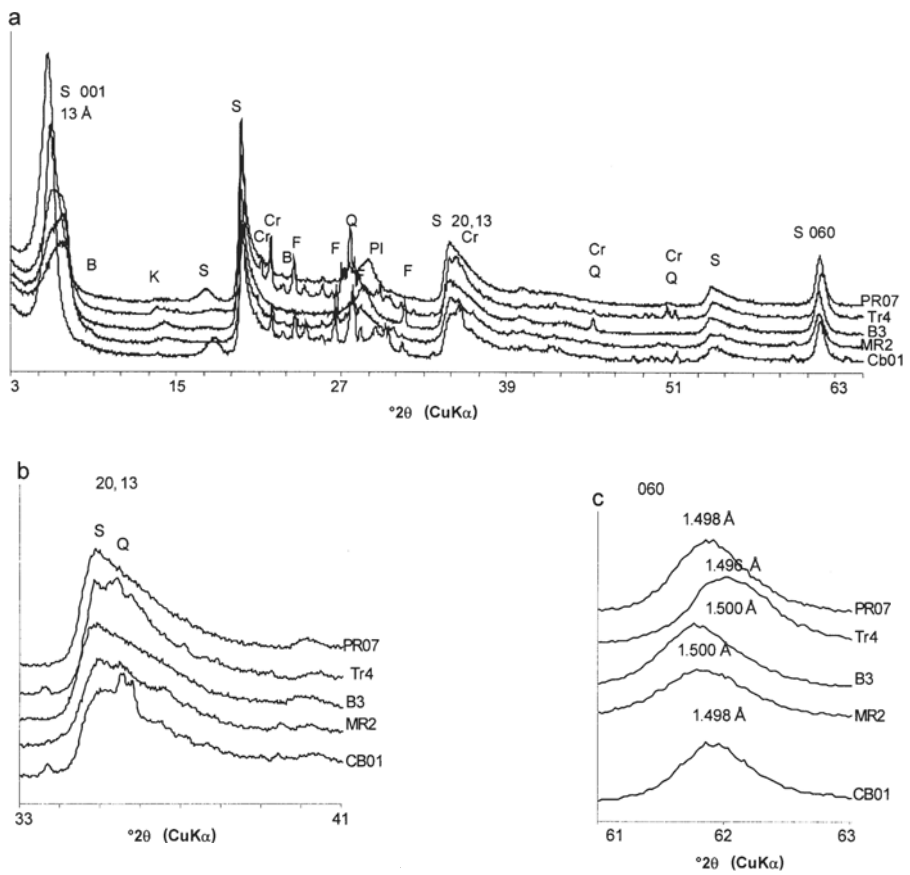

Figure 3. XRD patterns of randomly oriented powders of bulk rocks. (a) Clay minerals: smectite (S) and kaolinite (K) are associated with cristobatite (Cr) or quartz (Q), K-feldspar (F), Plagioclase (Pl), biotite (B). (b) The asymmetric 20,13 peak is typical of turbostratic layer stacking. (c) The 060 peak position is typical of dioctahedral smectites.

https://doi.org/10.1346/CCMN.2005.0530305 Published online by Cambridge University Press

Bulk-rock chemical composition

According to the Al and Mg contents, the bulk chemical analyses of representative samples from the five bentonite deposits can be separated into two groups (Table 2): PR07 and Tr4 bentonite samples are Al-rich and Mg-poor compared to B3, MR2 and CB01. All samples are depleted in silica compared to the non-argillized perlite. In spite of its 'fresh' aspect, the rhyolite sampled in the intrusive body at Providencia is severely hydrated and silica depleted compared to normal unaltered ones. Its composition (major and trace elements) is closed to that of the perlite (Table 2).

The *REE* distribution patterns normalized to CI chondrite (Evensen *et al.*, 1978) show that light elements (*LREE*) are more enriched than heavy ones (*HREE*) relative to CI chondrite in all the bentonite samples (Figure 4a). This is classically observed in clay deposits (Christidis, 1998, and references therein). The negative Ce anomaly typical of marine water alteration (Desprairies and Bonnot-Courtois, 1980) does not exist in the B3, MR2 and CB01 samples. Compared to the perlite *REE* pattern, two groups of samples can be distinguished (Figure 4b): (1) MR2 and B3: these samples are *REE* enriched, even in Eu in spite of the strong negative anomaly; (2) PR07, Tr4 and CB01: the *REE* patterns are similar to that of the perlite except for the heaviest *REE* (Er, Tm, Y and Lu) which are slightly depleted. The negative Eu anomaly is weak.

The element distribution patterns classified by their incompatibility degree (spider diagram normalized to the unaltered perlite) exhibit a similar shape whatever bentonite deposit is considered (Figure 4c). All are strongly depleted in Rb and Ba, the other elements being

Table 2. Bulk chemical compositions (major and trace elements) of the perlite, the unaltered obsidian (both sampled at Providencia), and the five bentonite samples.

	Rhyolite Tidiennit (P06)	Perlite Tidiennit (PR4)	Bentonite Providencia (PR07)	Bentonite Tribia (Tr4)	Bentonite Ibourhardayn (B3)	Bentonite Moulay Rachid (MR2)	Bentonite Melg el Ouidan (CB01)
(%)							
SiO_2	60.74	69.98	53.65	52.14	53.07	53.21	53.62
Al_2O_3	18.42	13.85	21.74	24.09	16.42	15.18	15.75
Fe_2O_3	0.78	1.17	2.15	1.58	2.03	3.2	2.88
MnO	<Id	0.05			0.05		
MgO	0.99	0.41	2.06	1.8	5.42	5.7	4.59
CaO	0.88	1.35	0.98	1.1	0.76	1.07	2.34
Na_2O	2.22	2.86	0.78	1.71	2.97	2.18	1.27
K_2O	4.1	3.99	0.35	0.54	0.54	0.69	0.52
TiO_2	0.12	0.11	0.2	0.14	0.12	0.21	0.5
P_2O_5	0.06	0.05	0.05	0.08	0.08	0.08	0.08
LOI	11.19	6.44	18.41	17.13	18.43	18.27	18.32
Total	99.5	100.26	100.37	100.31	99.89	99.79	99.87
(ppm)							
Rb	134	318	13.6	15.5	7.74	26.1	69
Ba	1468	1380	281	201	819	197	217
Th	33.6	29.2	48.1	69.3	37.4	33.3	10.3
Nb	18.6	14.7	23.1	11.7	14.6	19.8	13.3
Ta	1.87	1.56	2.74	2.1	1.59	1.87	1.11
La	34.2	29.4	20	33.8	46	51.6	29.3
Ce	65.2	55.9	44.2	71.1	80.1	87.9	57.8
Sr	131	195	103	126	97.1	110	195
Nd	22.1	18.9	15.5	24.1	32.5	37.7	23.6
Sm	3.9	3.34	2.86	4.14	5.78	6.59	4.35
Zr	245	300	198	262	179	202	143
Hf	7.47	7.91	5.86	8.26	5.44	5.79	3.86
Eu	0.808	0.705	0.534	0.562	0.763	0.813	0.962
Gd	2.85	2.53	2.03	2.69	4.36	4.6	3.58
Tb	0.448	0.401	0.347	0.412	0.68	0.714	0.541
Dy	2.68	2.47	2.23	2.33	4.03	4.05	3.18
Y	14.6	15.3	13.9	11.5	21.6	21.5	18.4
Er	1.57	1.59	1.42	1.18	2.31	2.3	1.85
Tm	0.253	0.28	0.228	0.178	0.366	0.362	0.284
Yb	1.71	2.07	1.53	1.15	2.64	2.59	2.01
Lu	0.259	0.338	0.229	0.183	0.403	0.403	0.309

https://doi.org/10.1346/CCMN.2005.0530305 Published online by Cambridge University Press

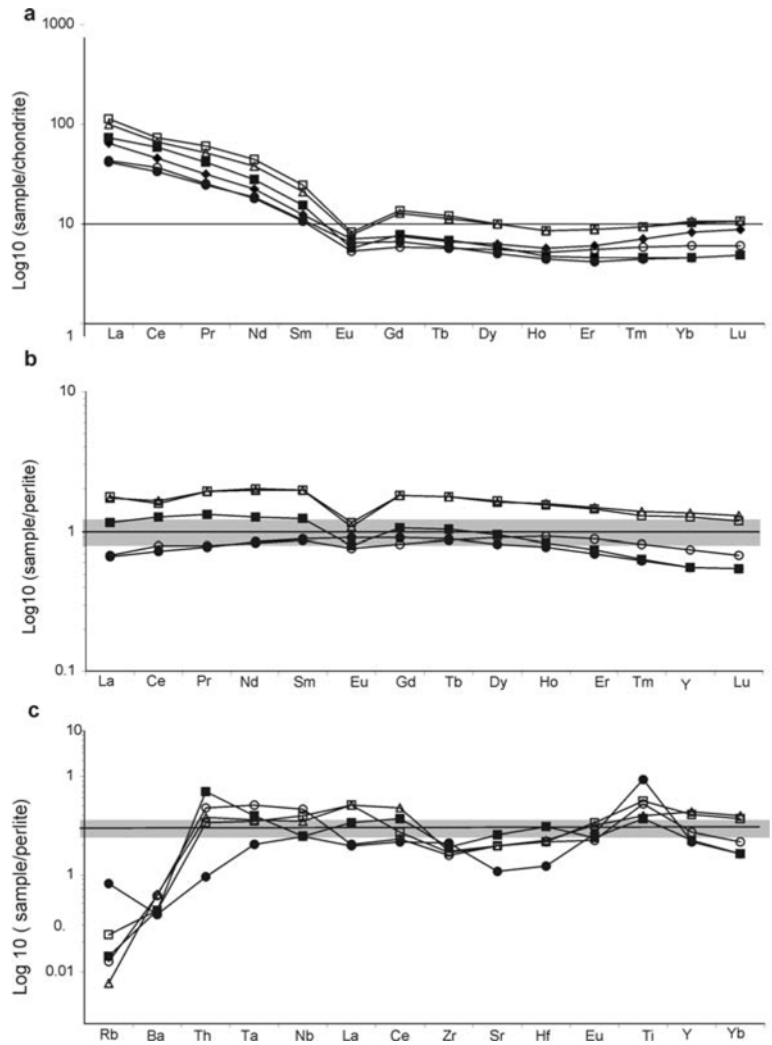

Figure 4. Chemical compositions of the bulk rocks. (a) Variation of *REE* normalized to CI chondrite. (b) Variation of *REE* normalized to the unaltered perlite. (c) Variation of incompatible element amounts normalized to the unaltered perlite. Open circle: PR07; filled square: Tr4; triangle: B3; open square: MR2; filled circle: CB01; filled diamond: perlite. The grey zone represents the estimated error envelope around the reference line.

nearer the reference line. The Rb and Ba depletion is related to alteration processes. The bentonite from CB01 is slightly depleted in Sr, Hf, Th and enriched in Ti, compared to the other samples.

Microprobe analyses

In spite of low totals (91–95.5%), the chemical composition of glass relics in the PR07 and Tr4 bentonites samples and in the altered pyroclastic flows from B3 is similar to that of an unaltered rhyolite (Table 3). The low totals probably result from hydration (water content not measured). The SiO_2 and K_2O contents are significantly higher than those measured in the perlite. According to the major chemical elements, two groups of smectites can be distinguished: PR07, Tr4 and B3, MR2, CB01 which are particularly rich in Al_2O_3 and MgO-Fe_2O_3, respectively. The structural formulae were calculated on the $O_{10}(OH)_2$ basis assuming that the number of interlayer Mg^{2+} cations is given by the excess octahedral occupancy (Table 3). The tetrahedral charge varies from 60 to 80% and from 6 to 10% of the total negative charge for the first and second group, respectively. Al-rich smectite (beidellite) is apparently formed preferentially in the hydrothermal alteration sites (PR07 and Tr4) while montmorillonite is preferentially formed in the volcano-sedimentary deposits (B3, MR2 and CB01). The mean interlayer charge varies from the low- to high-charge smectite poles: 0.3 to 0.6 per $O_{10}(OH)_2$.

Smectite crystallochemical characteritics

The XRD patterns of the Ca-saturated samples (oriented mounts) after ethylene glycol treatment are similar for the five samples (Figure 5). They are all characterized by a rational series of peaks (17 Å, 8.48 Å

https://doi.org/10.1346/CCMN.2005.0530305 Published online by Cambridge University Press

Table 3. Microprobe analyses of volcanic glass remains and clay minerals in the five bentonite deposits and structural formulae.

	Providencia (PR07)				Tribia (Tr4)				Ibourhardayn (B3)				Moulay Rachid (MR2)		Melg el Ouidan (CB01)	
	Gl (n = 10)		Cl (n = 9)		Gl (n = 7)		Cl (n = 13)		Gl (n = 5)		Cl (n = 7)		Cl (n = 9)		Cl (n = 8)	
	Mean	sd	Mean	sd	Mean	sd	Mean	sd	Mean	sd	Mean	sd	Mean	sd	Mean	sd
SiO_2	73.46	3.23	55.64	2.54	74.34	1.24	55.33	2.71	74.01	1	61.96	0.89	60.60	2.96	62.15	1.23
Al_2O_3	11.94	0.70	25.01	1.59	11.53	0.64	27.30	1.60	10.73	1.22	18.81	0.59	16.64	0.73	20.12	0.80
Fe_2O_3	0.45	0.43	1.83	0.62	1.04	0.16	1.88	0.28	0.52	0.5	3.84	0.99	3.39	0.95	3.14	0.50
MgO	0.06	0.03	1.91	0.31	0.07	0.02	1.29	0.29	0.05	0.02	5.74	0.77	7.37	0.38	4.90	0.32
MnO	0.07	0.06	0.05	0.00	0.12	0.10	0.01	0.03	0.05	0.06	0.02	0.04	0.04	0.08	0.06	0.06
CaO	0.51	0.22	0.81	0.47	0.76	0.08	1.24	0.33	0.50	0.19	0.09	0.04	0.35	0.10	1.04	0.38
Na_2O	2.43	0.46	1.34	0.36	2.69	0.31	0.76	0.22	2.01	0.43	1.71	0.29	2.17	0.14	0.46	0.41
K_2O	6.14	1.47	0.48	0.60	4.94	0.24	0.41	0.1	5.51	0.62	0.80	0.26	0.61	0.21	0.22	0.16
LOI	n.m.	n.m.	n.m.	n.m.	n.m.	n.m.	n.m.	n.m.	n.m.	n.m.	n.m.	n.m.	n.m.	n.m.	n.m.	n.m.
Total	95.04	2.63	87.05	4.00	95.48	1.35	88.24	3.56	93.39	2.66	92.98	1.19	91.16	4.10	92.34	1.79

Structural formulae based on $O_{10}(OH)_2$

	Providencia Mean (n = 9)	sd	Tribia Mean (n = 13)	sd	Ibourhardayn Mean (n = 7)	sd	Moulay Rachid Mean (n = 9)	sd	Melg el Ouidan Mean (n = 8)	sd
Si	3.76	0.06	3.68	0.08	3.95	0.03	3.96	0.03	3.96	0.02
^{IV}Al	0.24	0.06	0.32	0.08	0.05	0.03	0.04	0.03	0.04	0.02
^{VI}Al	1.75	0.05	1.82	0.05	1.37	0.02	1.24	0.02	1.47	0.02
Fe^{3+}	0.09	0.02	0.	0.01	0.18	0.05	0.17	0.03	0.16	0.01
^{VI}Mg	0.16	0.03	0.08	0.01	0.45	0.05	0.59	0.01	0.37	0.03
Mn	00	00	00	00	00	00	00	00	00	00
^{VI}cations	2.00		2.00		2.00		2.00		2.00	
Mg int.	0.03	0.03	0.05	0.03	0.10	0.01	0.12	0.02	0.09	0.01
Ca	0.04	0.03	0.08	0.02	0.01	0.003	0.03	0.01	0.07	0.03
Na	0.17	0.15	0.10	0.02	0.21	0.02	0.27	0.02	0.06	0.05
K	0.05	0.06	0.03	0.01	0.06	0.02	0.06	0.02	0.02	0.01
Tet. charge	0.24	0.06	0.32	0.08	0.05	0.03	0.04	0.03	0.04	0.02
Oct. charge	0.16	0.03	0.08	0.01	0.45	0.05	0.59	0.01	0.37	0.03
Layer ch.	0.4		0.4		0.5		0.63		0.41	
Interlayer ch.	0.36		0.39		0.49		0.63		0.4	

Gl: glass; Cl: clay; n: number of analyses; sd: standard deviation; int: interlayer; Tet.: tetrahedral; Oct.: octahedral; Ch: charge; LOI: loss on ignition; n.m.: not measured

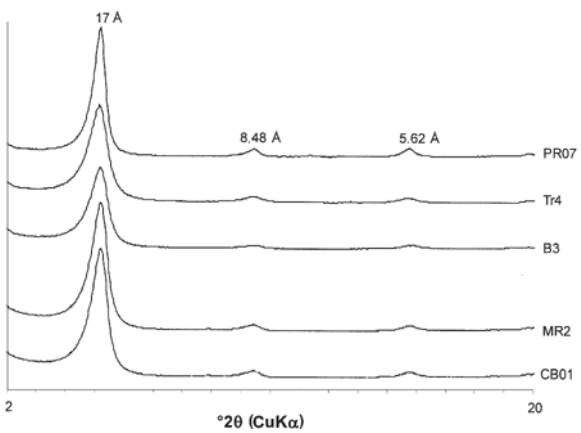

Figure 5. XRD patterns of Ca-saturated samples (<2 µm fraction) in the ethylene glycol-solvated state.

and 5.62 Å), typical of smectites having two glycol sheets in the interlayer space. However, the peak profiles are not identical: for PR07 and CB01, the 001 peak is symmetrical and sharp (FWHM <0.55°2θ). The background level in the low-angle region is low (saddle/peak value <0.1); for Tr4, B3 and MR2, the 001 peak is asymmetrical towards the low-angle region, broad (FWHM >0.62°2θ), and the background level higher (saddle/peak ratio >0.14).

The XRD patterns (oriented mounts) are strongly modified after K saturation (Figure 6a). The 001 reflection for all samples is less intense and broader (FWHM >1.13°2θ) than its equivalent in the Ca-saturated samples. The background level in the low-angle region increases (saddle/peak ratio >0.31). The 002 and 003 reflection harmonics are irrational and their intensity is extremely weak indicating a random interstratification of two or three different layers (Moore and

https://doi.org/10.1346/CCMN.2005.0530305 Published online by Cambridge University Press

Reynolds, 1989; Drits *et al*., 1997). From the comparison of XRD patterns obtained from Ca-EG and K-EG samples, it is possible to hypothesize the coexistence of expandable layers having contrasting charges and hydration properties (Meunier *et al*., 2004).

Two groups of samples can be distinguished according to the position of the 001 reflection and the saddle/peak ratio: for PR07, Tr4 and CB01, the position at 17.1−16.8 Å and the high saddle/peak ratio indicates a randomly ordered interstratification 2 EG−0 EG (10 Å collapsed) layers; for B3 and MR2, compared to the Ca-saturated samples, the position of the 001 reflection shifts to 14.7 and 15.5 Å, respectively. The saddle/peak ratio is high and the peaks are broad. This indicates interstratifications of fully (2 EG; 17 Å), partially (1 EG; 13.5 Å) and non-expandable layers (0 EG; 10 Å).

The XRD pattern decomposition shows that the broad intense peaks result from the contribution of different mixed-layer structures between 2 EG, 1 EG and 0 EG layers (Figure 6b).

Random 2- or 3-component mixed layers. The two more intense Gaussian curves whose positions vary from 17.3 to 18.9 Å and from 17.4 to 14.1 Å, respectively, are typical of randomly ordered mixed layers. The first is the contribution of the saddle/peak ratio (asymmetry in the

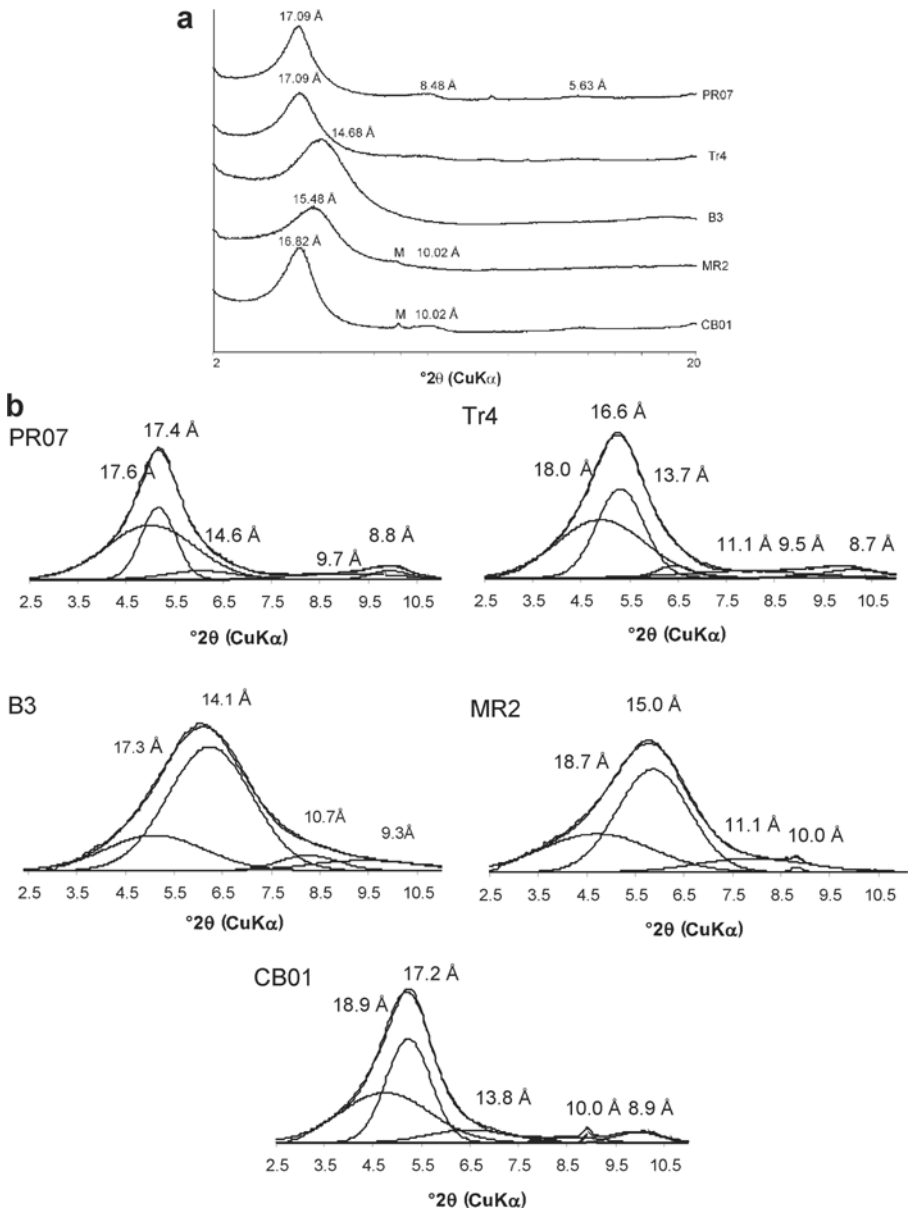

Figure 6. K-saturated samples (<2 μm fraction). (a) XRD patterns of oriented preparations in the ethylene glycol-solvated state. (b) Decomposition of the 001 and 002 peaks. M: biotite.

https://doi.org/10.1346/CCMN.2005.0530305 Published online by Cambridge University Press

low-angle range). The position of the second indicates what kind of layers are interstratified: 17.4 or 17.2 Å is typical of 2 EG−0 EG mixed layers (PR07 and CB01). The position remaining at ~17 Å indicates an interstratification similar to that of randomly-ordered illite-smectite (Moore and Reynolds, 1989). 16.6, 15.0 and 14.1 Å are theoretically typical of 2 EG−1 EG mixed layers (Tr4, B3 and MR2). However, because the second-order peak (8.5 to 9.7 Å) is absent or weak and very broad, it is probable that a third component (0 EG layer) is also interstratified (Drits *et al*., 1997; Claret *et al*. 2002; Calarge *et al*., 2003).

Ordered 2- or 3-component mixed layers. The broad and weak reflection from 14.6 to 10.7 Å probably corresponds to a partially ordered 3-component mixed layer.

In order to test the irreversible fixation of K^+ cations, the K samples were re-saturated with Ca^{2+} cations (K-Ca samples) and solvated with ethylene glycol. The XRD patterns of K-Ca samples (Figure 7a) show that all the samples re-expand to 17.0−17.1 Å but exhibit a higher saddle/peak ratio compared to Ca-saturated samples. Thus, the K saturation did not irreversibly collapse all the layers. Most recover their expandability when re-saturated with Ca. In other words, all the 1 EG and some of the 0 EG layers in the K-saturated samples become 2 EG layers in K-Ca samples. According to Sato *et al*. (1992), such differences in expandability are related to the layer charge. Using his data, one can distinguish three layer types: (1) 2 EG in K-saturated state – low-

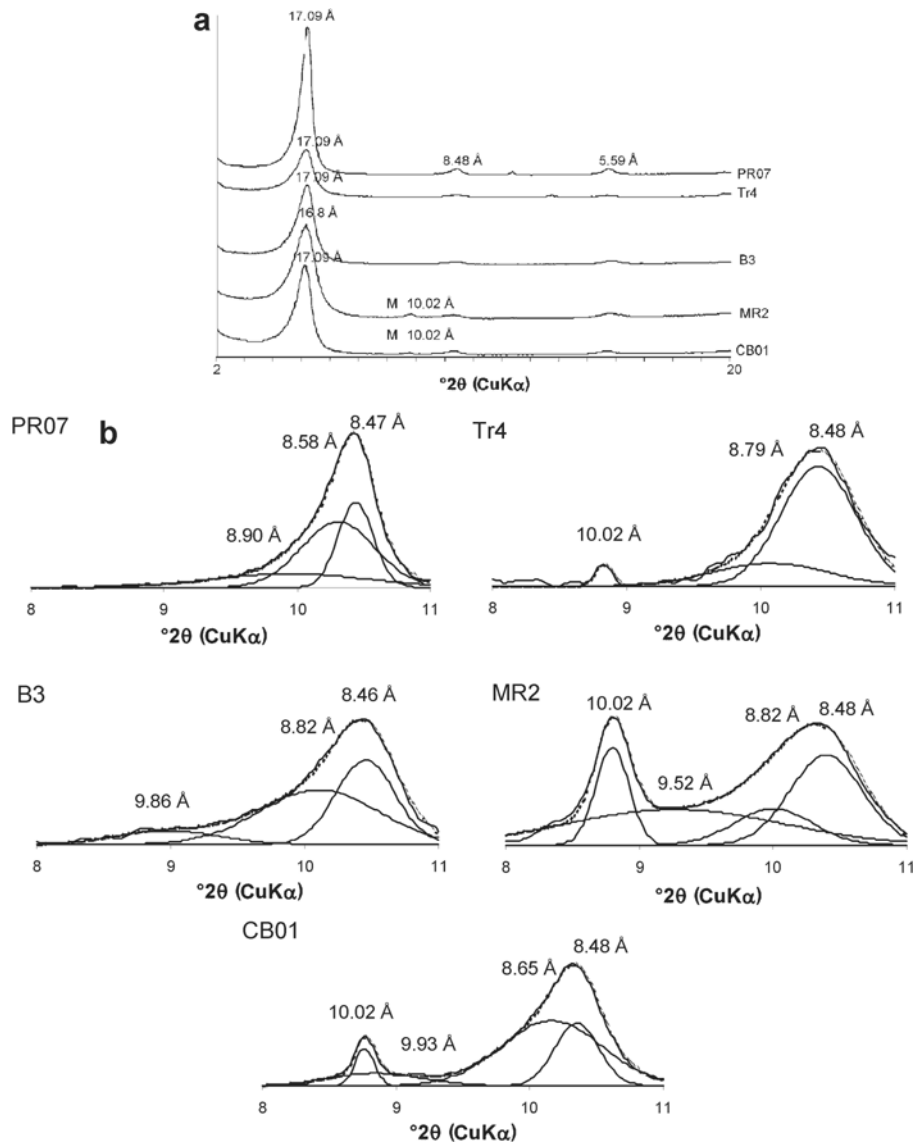

Figure 7. Ca-saturated K-samples (K-Ca; <2 μm fraction). (a) XRD patterns of the oriented patterns in the ethylene glycol-solvated state. (b) Decomposition of the 002 peak. M: biotite.

https://doi.org/10.1346/CCMN.2005.0530305 Published online by Cambridge University Press

Table 4. Cation exchange capacity (meq/100 g) of the <2 μm fraction measured on K- or K-Ca samples. The exchangeable Mg^{2+} and K^+ cation amounts are measured after exchange with NH_4^+. % $\Delta CEC_{(Ca-K)} = ((CEC_{Ca}-CEC_K)/CEC_{Ca}) \times 100$: % $\Delta CEC_{(Ca-K-Ca)} = ((CEC_{Ca}-CEC_{K\text{-}ca})/CEC_{Ca}) \times 100$.

	Providencia (PR07)	Tribia (Tr4)	Ibourhardayn (B3)	Moulay Rachid (MR2)	Melg el Ouidan (CB01)
Ca-saturated CEC	94.4	87.4	107.7	100.1	81.9
K-saturated CEC	76	68.7	87.3	77.2	70
K-Ca-saturated CECs	93.3	76.1	107.3	84.6	77
%Δ $CEC_{(Ca-K)}$	19	21	19	23	14
%Δ $CEC_{(Ca-K-Ca)}$	1	13	0.3	15	6
CEC_{Tetr}	47.3	65	18.5	19.9	13.1
$\%CEC_{Tetr}$	50	75	17	20	16
Exchangeable Mg	22.1	27.5	36.1	34.9	35
Exchangeable K	2.54	6.93	5.23	7.35	2.69

charge layers; (2) 0 EG after Ca resaturation – high-charge layers; and (3) 1 EG or 0 EG in the K-saturated state expanding to 2 EG after Ca resaturation – intermediate-charge layers.

The way that these three types of layers are interstratified in the K-Ca samples may be investigated by decomposition of the 002 peak which is asymmetric towards the low-angle region (Figure 7b). The decomposition shows that it is always composed of two or three elementary Gaussian curves having contrasted intensity and FWHM values. Plançon and Drits (2000) showed that the intensity and FWHM of second-order diffraction peaks are strongly modified by the presence of a third component in the interstratification. This peak becomes broad and much less intense. According to these results, the elementary reflections of the decomposed 002 diffraction peak can be interpreted as follows: 8.46 to 8.48 Å – FWHM = 0.31 to 0.66°2θ: fully expandable smectite – 2 EG layers; 8.58, 8.82 and 8.65 Å – FWHM = 0.65 to 0.89°2θ: random 0 EG–2 EG mixed layers in which the 2 EG layers are dominant; 8.79 and 8.90 Å – FWHM = 1.03 and 1.41°2θ: random 0 EG–1 EG–2 EG mixed layers in which the 2 EG layers are dominant; 9.52 and 9.93 Å – FWHM = 1.89 and 0.80°2θ: ordered 0 EG–1 EG–2 EG mixed layers in which the 0 EG layers are dominant.

Localization of the layer charge (Hofmann-Klemen treatment)

The expandability of smectites in which the octahedral charge was neutralized (Hofmann-Klemen treatment) has been investigated for the five bentonite samples. Three types of XRD patterns can be distinguished (Figure 8): PR07, Tr4 – the 17 Å and 8.48 Å peaks are typical of beidellite; MR2, CB01 – the 9.68 Å peak is typical of montmorillonite; B3 – the 9.55 and 17.1 Å peaks correspond to two different coherent diffracting domains typical of random mixed-layer structures composed of 2 EG beidellic layers interstratified with collapsed montmorillonitic ones, respectively. The 9.55 Å peak indicates that the montmorillonitic layers are dominant while the 17.1 Å reflection, in spite of its relatively high saddle/peak ratio, indicates that beidellitic layers are dominant.

CEC and exchangeable cations

The CEC_{total} (samples in the Ca-saturated state) varies from 81.9 to 107.7 meq/100 g, typical of smectites (Table 4). After neutralization of the octahedral charge using the Hofman-Klemen treatment, the CEC decreases and values range from 65.01 to 13.1 meq/100 g according to the sample considered. These values represent the CEC linked to tetrahedral charges (CEC_{tetr}). As expected, CEC_{tetr} is much higher in the beidellitic clays (PR07 and Tr4) than in the montmorillonitic ones (MR2 and CB01). In spite of the presence of a beidellitic component identifiable in the XRD patterns of the Li-treated samples (Figure 8), the B3 sample has a CEC_{tetr} equivalent to that of pure montmorillonitic samples without beidellitic layers. On the other hand, the layer charge of the PRO 7 sample which yields a pure beidellitic signal originates for 40% in the octahedral sheet. This means that the swelling property for a given layer after Li treatment is maintained even if a limited proportion of the layer

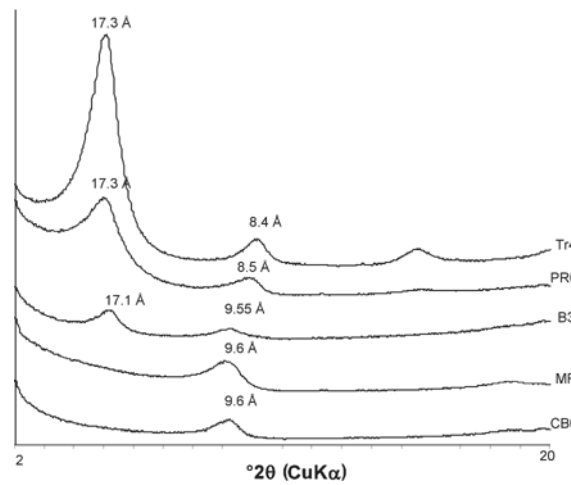

Figure 8. XRD patterns of the <2 μm fractions after Hofmann-Klemen treatment.

https://doi.org/10.1346/CCMN.2005.0530305 Published online by Cambridge University Press

charge is located in the tetrahedral sheet. The collapse to 9.6 Å is related solely to montmorillonitic layers. The CEC_{total} and CEC_{tetr} increase proportionally to layer charge in a limited range (to 0.5 per $O_{10}(OH)_2$) (Figure 9).

For all the samples, the CEC decreases from 14 to 23% after K saturation. This decrease depends on the number of sites which strongly fix the K^+. If these sites are located in specific layers (high-charge layers), then the expandability of the smectite is reduced (Figure 6). After Ca saturation of the K-samples, the CEC increases indicating that most of the sites in the interlayer region recovered their exchangeability. Concomitantly, the expandability of the smectite is totally or partially restored. The loss of CEC during the K-Ca two-stage saturation procedure varies from 0 to 15% which reflects the percentage of the sites which irreversibly lost their exchangeability. In that case, the XRD patterns of the Ca- and K-Ca-saturated samples are not similar (Figure 7a)

The exchangeable cations were determined on the untreated samples in order to avoid a possible chemical contamination of the <2 μm fraction during the extraction procedure. Abnormally high Na^+ and Ca^{2+} amounts have been observed in the bentonite samples probably due to the presence of undetected calcite, halite or gypsum impurities. Such contamination does not affect the determination of the Mg^{2+} and K^+ exchangeable cations, which are more closely representative of the clay fraction. Despite the fact that the concentration of Mg and K is smaller compared to the interlayer composition given in the mean structural formulae (Table 2), it is confirmed that Mg^{2+}, Ca^{2+}, K^+ and Na^+ cations are present in the smectite interlayers.

DISCUSSION

Among the parameters which may influence the crystallochemical characteristics of smectites in bentonite deposits, two must be given priority: the chemical composition of the volcanic glass and the composition of the solutions in which alteration took place. The other parameters, such as temperature conditions and water/rock ratio cannot be ignored but they do not control the crystallographic properties of the clays. They influence only the reaction kinetics.

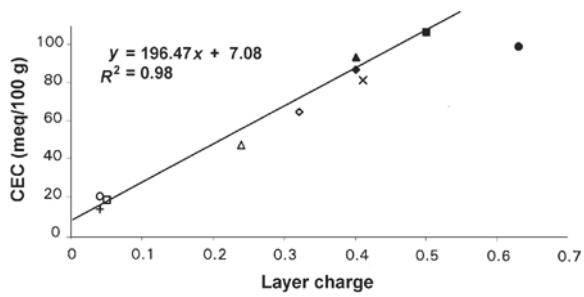

Figure 9. Relationship between the layer charge of untreated and Hofmann-Klemen (H-K)-treated samples and the CEC. Filled triangle: untreated-PR07; open triangle: H-K-treated PR07; filled diamonds: untreated Tr4; open diamonds: H-K-treated Tr4; filled square: untreated B3; open square: H-K-treated B3; filled circle: untreated MR2; open circle: H-K-treated MR2; ×: untreated CB01; +: H-K-treated CB01.

Table 5. La/Yb, Nb/Ta and Zr/Hf ratios for the five bentonite samples and the perlite and rhyolite from Providencia.

Sample	La/Yb	Nb/Ta	Zr/Hf
Perlite PR4	14.20	9.42	37.93
Rhyolite P06	20.00	9.95	32.8
PR07	13.07	8.43	33.79
TR4	29.39	5.76	31.72
B3	17.42	9.18	32.90
MR2	19.92	10.59	34.87
CB01	13.95	11.98	37.93

Composition of the volcanic glass

Because the temperature of the volcanic ashes when falling in water is unknown, the rate at which the glass is converted into smectite in natural environments is highly variable: from a few hours or days (Berry, 1999) to a few years (Davies *et al.*, 1979; Zielinski, 1980). However, the recrystallization process is rapid compared to the immobile element redistribution during water/rock interactions (Zielinski, 1982, 1985). Consequently, it is possible to estimate the composition of the original volcanic glass on the basis of ratios of relatively immobile elements in the bulk bentonite rock (smectite + accessory minerals). Such attempts at chemical fingerprinting have had mixed success because alteration processes have been shown to modify the relative proportions of most elements to various degrees (Christidis, 1998). However, the La/Yb, Nb/Ta, Zr/Hf ratios (Table 5) of the bentonites derived from the alteration of volcanic ashes (B3, MR2, CB01) are close to that of the rhyolite. Plotted in the Zr-Nb-Ta system (Figure 10), their compositions are closer to that of rhyolite than to that of the bentonites produced by the alteration of the volcanic glass inside the volcano (Pr07 and Tr4).

Despite the potential limitations of chemical fingerprinting techniques, *REE* patterns presented in Figure 4 show a strong compositional similarity between the perlite of the Tidiennit Massif and the five measured bentonites of different geological settings. When normalized to the perlite, the abundance of *REE* and incompatible elements in the five bentonite samples are sufficiently close to the perlite reference line to permit a perlite-like original composition. No other normalization using andesite, latite or dacite references is closer to that of the perlite. The La/Yb, Nb/Ta and Zr/Hf ratios for the five bentonites (Table 5) are very close to that of the perlite or the rhyolite sampled in the Providencia volcano. Consequently, it is very likely that the five

https://doi.org/10.1346/CCMN.2005.0530305 Published online by Cambridge University Press

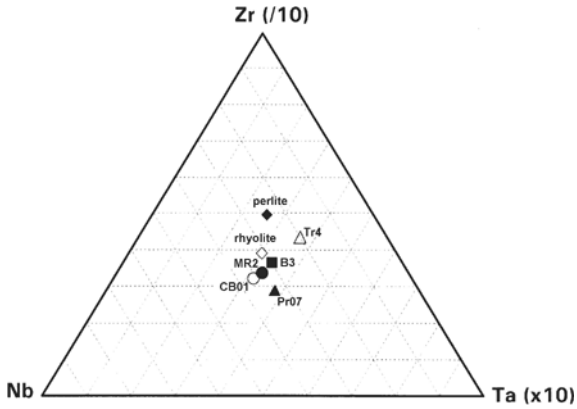

Figure 10. Plot of the chemical compositions of the bentonites and the rhyolite and perlite samples in the Zr-Nb-Ta system. For clarity, the Zr and Ta amounts were divided or multiplied by 10, respectively.

bentonites originate from volcanic glasses typical of rhyolitic magmas.

However, the amounts of some elements are significantly different in the bentonites compared to the perlite. (1) The negative Eu anomaly is marked in the Tr4, B3 and MR2 samples. This is related to the degree of plagioclase crystallization in the magma before the volcanic glass is formed. (2) There is a consistent, strong depletion of Rb and Ba and, to a lesser extent, Sr in all the samples. The depletion could be related either to the crystallization of K-feldspar and biotite (differentiation) or to the alteration processes because of the geochemical mobility of alkali and alkaline earth elements during water/rock interactions.

The variation of the negative Eu anomaly and the Rb, Ba and Sr depletion indicate that the bentonites were not formed from a unique volcanic glass composition. Consequently, it is highly probable that the parent pyroclastics and ashes do not originate from a single eruption event but probably from several during a period long enough for the magma to differentiate inside the magmatic chamber.

Smectite layer-charge heterogeneities

The principal XRD and chemical characteristics of the smectite forming the bentonite deposits are summarized in Table 6. The average layer charge of the smectites varies from 0.40 to 0.63 per $O_{10}(OH)_2$. However, the average values do not signify that all the layers are similarly charged. The magnitude and location of charge may vary as indicated by the differences between the XRD patterns of samples after Ca, K or K-Ca saturations or Li treatment.

According to the response to the Li treatment, three types of smectite can be distinguished: beidellite (PRO7, Tr4), beidellite-montmorillonite (B3) and montmorillonite (MR2, CB01). The B3 sample, in spite of the small contribution of tetrahedral substitutions to the layer charge (Table 3), remains partially expandable after the Li treatment. This indicates that the tetrahedral charge is not homogeneously shared among all the layers but preferentially located in some of them. These layers form coherent scattering domains sufficiently large to diffract X-rays (17.1 Å peak). The other layers have no tetrahedral charge and collapse to 9.6 Å.

The comparison of XRD patterns from Ca-, K- and K-Ca-saturated samples indicates that all the layers in a given smectite sample do not have the same charge. This heterogeneity is particularly evident in samples PR07 and Tr4 both of which are beidellites, and which have nearly identical average layer charge, *i.e.* $\approx$ 0.40 per $O_{10}(OH)_2$. However, the decomposition of the 002 peak from the K-saturated samples (Figure 6b) shows that the swelling properties are not identical. The presence of partially or non-expandable layers militates for interlayer charge heterogeneities. There is no correlation between their presence and the mean layer charge or the residual CEC (Table 5). The interlayer swelling is controlled by the value and the location of the layer charge (Sato *et al.*, 1992). According to their chemical characteristics, the smectites present both tetrahedral and octahedral charge, even if their XRD patterns after

Table 6. Summary of the XRD and chemical characteristics of the smectites in the five bentonite deposits.

	XRD properties		H-K	Mean layer charge	$CEC_{Ca}-CEC_{K-Ca}$	% CEC lost
	001 K-sat	002 K-Ca sat				
PR07	17 Å–R0 2 EG–0 EG	8.48–6 8.58 Å Sm + R0 (2 EG 95%)	Beid	0.40	1.1	1
Tr4	16.6 Å–R0 2 EG–1 EG–0 EG	8.48–8.78 Å Sm + R0 (2 EG 75%)	Beid	0.40	11.3	13
B3	14.7 Å–R0 2 EG–1 EG–0 EG	8.48–8.82 Å Sm + R0 (2 EG 70%) 9.86 Å R1 (2 EG 10%)	Beid+Mont	0.50	0.4	0.3
MR2	15.0 Å–R0 2 EG–1 EG–0 EG	8.48–8.82 Å Sm + R0 (2 EG 70%) 9.52 Å R1 (2 EG 15%)	Mont	0.63	15.5	15
CB01	17 Å–R 0 2 EG – 0 EG	8.48–8.85 Å Sm + R0 (2 EG 68%) 9.93 Å R1 (2 Eg 5%)	Mont	0.41	4.9	6

H-K: Hofmann-Klemen

https://doi.org/10.1346/CCMN.2005.0530305 Published online by Cambridge University Press

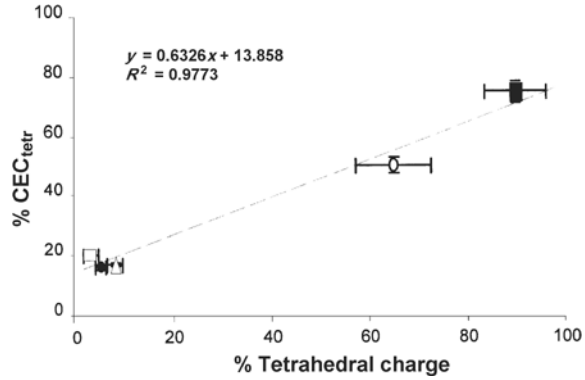

Figure 11. Relationship between the tetrahedral charge and the remaining CEC after H-K treatment. Tetrahedral charge and remaining CEC are expressed as a percent of total layer charge and total CEC, respectively.

Li treatment are typical of pure beidellites or montmorillonites. This is confirmed by the CEC_{tetr} measurements which show that tetrahedral charges contribute to CEC_{total} even in the most montmorillonitic clay samples (B3, MR2 and CB01). The tetrahedral charge (% of layer charge) is correlated to the $\%CEC_{tetr}$ (Figure 11).

Alteration processes

The glass relics in the bentonite beds, in spite of hydration, have a chemical composition close to that of an unaltered rhyolite. This is not the case for the perlite and the rhyolite samples from Providencia which are more hydrated and silica depleted. As shown by the Al_2O_3 *vs.* SiO_2 plot (Figure 12), the composition of the perlite is intermediate between unaltered glass and bentonites. Thus, the SiO_2/Al_2O_3 ratio may be used as a variable indicating the intensity of the chemical transformation of the volcanic glass during argillization.

Compared to the distal volcanic glass and the perlite, the smectites originating from alteration are silica depleted and Mg enriched. Both characteristics are observed repeatedly both in natural environments (Christidis, 1998, and references therein) and in closed experimental systems (De La Fuente *et al.*, 2000). Examining the variation of MgO and Fe_2O_3 *vs.* SiO_2/Al_2O_3 (Figure 13a,b) shows two chemical trends according to the type of environment: hydrothermal veins (PR07, Tr4) – shallow-sloped trend line; and, sedimentary formations (B3, MR2, CB01) – sharp-sloped trend line.

In all cases, K is almost completely leached out of the glass by the hydration and clay-formation processes (Figure 13c); only a small amount remains adsorbed in the exchangeable sites of the smectites (Table 3).

The glass to smectite reaction releases silica in amounts that should yield quartz or secondary opal. This is the case in the alteration of the glass shards of the Otay bentonite from California (Berry, 1999). In Morocco, the excess silica is consumed by the crystallization of cristobalite forming spherolites (see Figure 3). When plotted in the M^{+}-4Si-R^{2+} coordinates

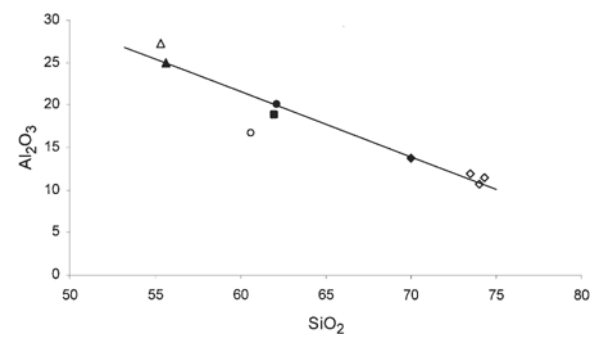

Figure 12. Variation of the chemical composition of bulk rocks by alteration. The amount of Al_2O_3 increases linearly with decreasing SiO_2. Open diamond: rhyolite glass; filled diamond: perlite; triangle: Tr4; filled triangle: PR07; open circle: MR2; filled circle: CB01; filled square: B3.

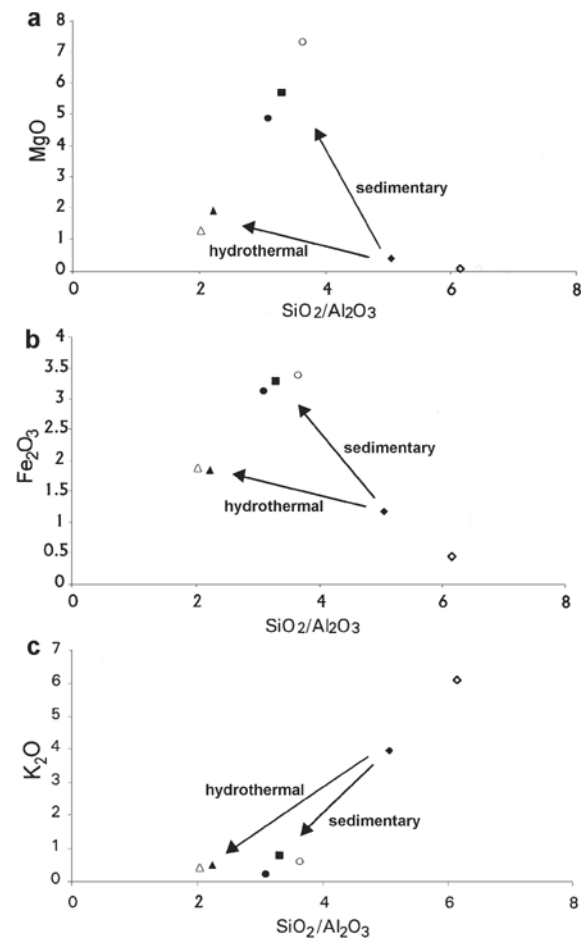

Figure 13. Variation of the chemical composition of bulk rocks. The MgO (a) and Fe_2O_3 (b) amounts increase differentially according to two chemical trends. (c) The K is almost completely lost. Open diamond: rhyolite glass; filled diamond: perlite; open triangle: Tr4; filled triangle: PR07; open circle: MR2; filled circle: CB01; filled square: B3.

https://doi.org/10.1346/CCMN.2005.0530305 Published online by Cambridge University Press

(Meunier and Velde, 1989; here, M^+ = K^++Na^++2Ca^{2+},4Si = Si/4, R^{2+} = Mg^{2+}), the smectites form two groups (Figure 14a): one in between the montmorillonite and beidellite regions (PR07, TR4) and the other near the montmorillonite region (MR2, B3, CB01). The compositions in the first group are similar to that of the beidellites formed in the boiling zone of the Bouillante active geothermal field (Patrier *et al*., 2003) or in Milos Island (Christidis and Dunham, 1997). All have been determined as beidellites (Figure 14b,c) and were formed in an open chemical system where the alteration processes are controlled by the fluid composition.

Conversely, the compositions in the second group are similar to that of smectites from Kimolos Island (Figure 14c) which are associated with zeolites (Christidis, 2001). All are very close to the montmorillonite region. Even if zeolites are absent from the Moroccan bentonites, one can consider that the smectites are formed in a nearly closed chemical system. The argillization process of the rhyolite glass is similar to that reproduced in the experimental alteration of the Cabo de Gata perlite (De La Fuente, 2000) which produces smectite and illite-smectite mixed-layer minerals (Figure 14d).

The separation of the beidellite and montmorillonite obviously depends on the amount of Mg available in the alteration system. This element may be provided either by the volcanic glass and/or the altering solutions. In active hydrothermal zones where the solutions invading the rocks are Mg depleted because of the previous crystallization of Mg silicates deeper, in higher temperature zones. Beidellites are formed in the Bouillante geothermal field in spite of a Mg-rich context (andesite basalts, sea-water). On the contrary, the montmorillonitic smectites are formed at surface conditions in marine, lagoonal, even lacustrine environments in which the alteration systems were nearly closed, the solutions being resident in the pores of the rocks. Under such conditions, the Mg uptake by the phyllosilicate phases

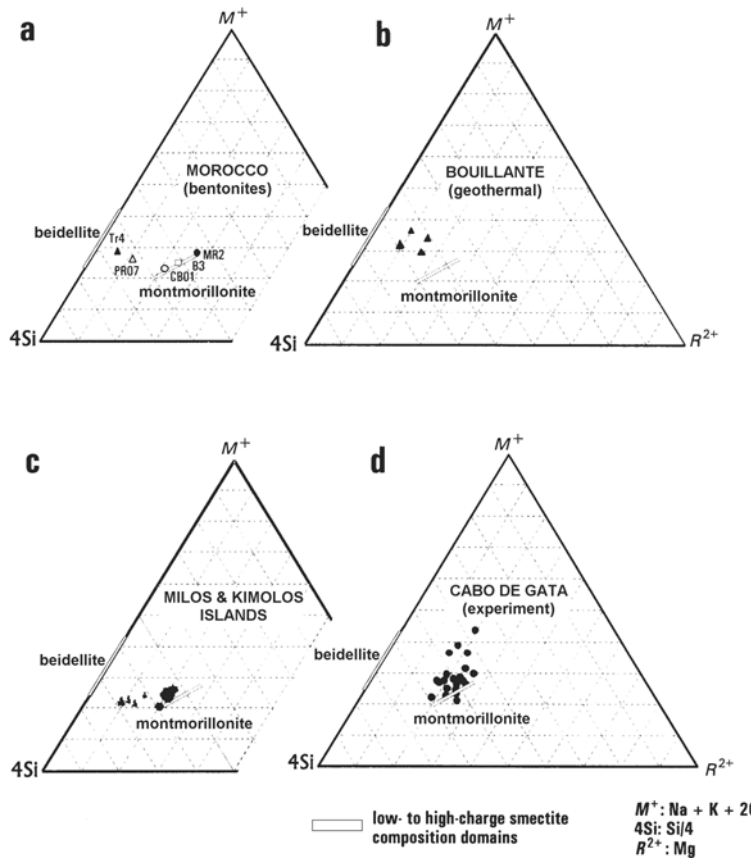

Figure 14. Comparison of clay mineral composition formed by rhyolite glass (a, c and d) and andesite glass (b) alteration. (a) Bentonites from northern Morocco. Filled triangle: beidellite (PR07 and Tr4); filled circle: montmorillonite (B3; MR2, CB01). (b) Beidellite (filled triangle) formed in the hydrothermal system of Bouillante, Guadeloupe, French West Indies (data from Patrier *et al*., 2003). (c) Bentonites formed by rhyolite glass in hydrothermal activity from Milos Island (data from Christidis and Dunham, 1997) and from Kimolos islands (data from Christidis, 2001). (d) Experimental alteration of the rhyolite glass from Cabo de Gata; southern Spain (data from De la Fuente *et al*., 2000). Filled circle: montmorillonite. Filled triangle: beidellite and Al-rich montmorillonite; filled circle: Chambers and Tatatilla type montmorillonite.

https://doi.org/10.1346/CCMN.2005.0530305 Published online by Cambridge University Press

was sufficient to produce nearly pure montmorillonitic clays from volcanic ash deposits in the Moulay Rachid and Melg el Ouidan deposits. Magnesium may be provided by the solutions (sea or lagoonal-lacustrine waters) and the rhyolite glass itself as is the case in the alteration experiments.

The Ibourhardayn bentonite which is composed of both beidellite and montmorillonite could result from two different argillization processes. As it was formed near (5 km) the volcano, from a pyroclastic flow, the beidellite could be inherited from a previous hydrothermal alteration event of the rhyolite glass inside the volcano similar to that observed in Providencia or Tribia. Then, when in contact with sea or lagoonal water, Mg^{2+} cations are absorbed in the interlayer exchangeable sites and not incorporated within the octahedral sheet (Mg-beidellite). Concomitantly, the fresh glass fragments are transformed into montmorillonite according to an argillization process similar to that operating in the Moulay Rachid and Melg el Ouidan deposits.

CONCLUSIONS

The bentonite deposits of northern Morocco studied here originate from similar sources of rhyolitic glass. However, the differences in the *REE* patterns normalized to the perlite indicate that the bentonites were not formed after a single eruption event but probably over a longer period of volcanic activity during which the magma differentiated inside the magmatic chamber. The Rb and Ba depletion in spider diagrams as well as the negative Eu anomaly in the *REE* patterns are related to that differentiation process.

Smectites formed from the rhyolitic glass when it interacted with water in environments as different as hydrothermal systems inside the volcanoes, and marine or lagoonal-lacustrine sediments at different distances from the eruptive center. No zeolite has been detected but the crystallochemical composition of the smectites varies with the local conditions of the argillization process: they are beidellitic in hydrothermal systems and montmorillonitic in marine or lagoonal-lacustrine sediments. The most montmorillonitic clays originate from ashes transported few tens of kilometers away from the volcanic center. A mixed beidellite-montmorillonite clay is found in pyroclastic flow deposited in sea-water close to the volcano.

All the smectites have both tetrahedral and octahedral charge, even if their XRD patterns after Li treatment are typical of pure beidellites or montmorillonites. The CEC, linked to the tetrahedral charges (CEC_{tetr}), is never zero even in the most montmorillonitic clay samples (MR2 and CB01). The average layer charge of the smectites varies independently of the location of negative charges in the 2:1 layers. The charge distribution is heterogeneous as indicated by the loss of expandability and the decrease in CEC after K-Ca treatment. This means that some layers are charged enough to fix K irreversibly whatever the average layer charge.

ACKNOWLEDGMENTS

Financial support for this work was provided by the Action Intégrée Franco-Marocaine N° MA/01/12. The authors are greatly indebted to R.A. Zielinski, G. Christidis and an anonymous referee for their helpful suggestions. We warmly thank Dr Crawford Elliott whose suggestions greatly improved the manuscript.

REFERENCES

Ait Brahim, L (1991) Tectoniques cassantes et états de contraintes récentes au Nord du Maroc. PhD thesis, Université Mohammed V Rabat, Morocco, 233 pp.

Benson, R.H., Rakic-El-Bied, K. and Bonaduce, G. (1991) An important current reversal (influx) in the Rifain corridor (Morocco) at the Tortonian-Messinian Boundary: the end of Tethys ocean. *Paleoceanography*, **6**, 164–192

Berry, R. (1999) Eocene and Oligocene Otay-type waxy bentonites of San Diego county and Baja California: chemistry, mineralogy, petrology and plate tectonic implications. *Clays and Clay Minerals*, **47**, 70–83.

Boles, J.R. and Surdam, R.C. (1979) Diagenesis of volcanogenic sediments in a Tertiary saline lake, Wagon Red Formation. *American Journal of Science*, **279**, 832–853.

Calarge, L., Lanson, B., Meunier, A. and Formoso, M.L. (2003) The smectitic minerals in a bentonite deposit from Melo (Uruguay). *Clay Minerals*, **38**, 25–34.

Christidis, G. (1998) Comparative study of the mobility of major and trace elements during alteration of an andesite and a rhyolite to bentonite, in the islands of Milos and Kimolos, Aegean, Greece. *Clays and Clay Minerals*, **46**, 379–399.

Christidis, G. (2001) Formation and growth of smectites in bentonites: a case study from Kimolos island, Aegean, Greece. *Clays and Clay Minerals*, **49**, 204–215.

Christidis, G. and Dunham, A.C. (1993) Compositional variations in smectites: Part I. Alteration of intermediate volcanic rocks. A case study from Milos Island, Greece. *Clay Minerals*, **28**, 255–275.

Christidis, G. and Dunham, A.C. (1997) Compositional variations in smectites: Part II: Alteration of acidic precursors. A case study from Milos Island, Greece. *Clay Minerals*, **32**, 253–270.

Claret, F., Bauer, A., Schäfer, T., Griffault, L. and Lanson, B. (2002) Experimental investigation of the interaction of clays with high pH solutions: a case study from the Callovo-Oxfordian formation, Meuse-Haute Marne underground laboratory (France). *Clays and Clay Minerals*, **50**, 633–646.

Davies, D.K., Almon, W.R., Bonis, S.B. and Hunter, B.E. (1979) Deposition and diagenesis of Tertiary-Holocene volcaniclastics, Guatemala. *SEPM Special Publication*, **26**, 281–306.

De La Fuente, S., Cuadros, J., Fiore, S. and Linares, J. (2000) Electron microscopy study of volcanic pyroclastic flow alteration to illite-smectite under hydrothermal conditions. *Clays and Clay Minerals*, **48**, 339–350.

Desprairies, A. and Bonnet-Courtois, C. (1980) Relation entre la composition des smectites d'altération sous-marine et leur cortège de terres rares. *Earth and Planetary Science Letters*, **48**, 124–130.

Drits, V.A., Lindgreen, H., Sakharov, B.A. and Salyn, A.S. (1997) Sequence structure transformation of illite-smectite-vermiculite during diagenesis of Upper Jurassic shales,

North Sea. *Clay Minerals*, **33**, 351–371.

Duggen, S., Hoernle, K., Bogaard, van den P. and Harris, C. (2004) Magmatic evolution of the Alboran region: The role of subduction in forming the western Mediterranean and causing the Messinian Salinity Crisis. *Earth and Planetary Science Letters*, **218**, 91–108.

El Bakkali, S. (1995) Volcanologie et magmatologie du système du Gourougou (Rif oriental, Maroc). PhD thesis, Univertité Blaise Pascal, Clermont-Ferrand II, France, 283 pp.

Evensen, G.R., Hamilton, P.J. and O'Nions, R.K. (1978) Rare-earth abundances in chondritic meteorites. *Geochimica et Cosmochimica Acta*, **42**, 1199–1212.

Fiore, S. Huertas, F.J., Huertas, J. and Linares, J. (2001) Smectite formation in rhyolite obsidian as inferred by microscopic (SEM-TEM-AEM) investigation. *Clay Minerals*, **36**, 489–500.

Hein, J.R. and Scholl, D.W. (1978) Diagenesis and distribution of late Cenozoic volcanic sediments in the southern Bering Sea. *Geological Society of America Bulletin*, **89**, 197–210.

Grim, R.E. and Güven, N. (1978) *Bentonites, Geology, Mineralogy, Properties and Uses*. Developments in Sedimentology, **24**, Elsevier, Amsterdam, 256 pp.

Hernandez, J. (1983) Le volcanisme Miocène du Rif Oriental (Maroc): Géologie, pétrologie et minéralogie d'une province shoshonitique. PhD thesis, Université Pierre et Marie Curie, Paris VI, France, 592 pp.

Hernandez, J. (1986) Pétrologie du massif volcanique de Guiliz (Maroc Oriental): Cristallisation fractionnée, mélange de magmas et transferts de fluides dans une série shoshonitique. *Journal of African Earth Sciences*, **5**, 4, 381–399.

Hofmann, U. and Klemen, R. (1950) Verlust der Austauschfähigkeit von Lithiuminonen an bentonit durch Erhitzung. *Zeitschrift für Anorganische und Allgemeine Chemie*, **262**, 95–99.

Huertas, F.J., Cuadros, J., Huertas, F.and Linares, J. (2000) Experimental study of the hydrothermal formation of smectite in the beidellite-saponite series. *American Journal of Science*, **300**, 504–527.

Huff, W.D., Anderson, T.B., Rundle, C.C. and Odin G.S. (1991) Chemostratigraphy, K-Ar ages and illitization of Silurian K-bentonites from the Central Belt of the Southern Uplands-Down-Longford terrane, British Isles. *Journal of the Geological Society*, 148, 861–868.

Imbert, T. and Desprairies, A. (1987) Neoformation of halloysite on volcanic glass in a marine environment. *Clay Minerals*, **31**, 81–91.

Inoue, A., Bouchet, A., Velde, B. and Meunier, A. (1989) A convenient technique to estimate smectite layer percentage in randomly interstratified illite/smectite minerals. *Clays and Clay Minerals*, **37**, 227–234.

Keller, J., Ryan, W.B.F., Ninkovich, D. and Altherr, R. (1978) Explosive volcanic activity in the Mediterranean over the past 200,000 y as recorded in deep-sea sediments. *Geological Society of America Bulletin*, **89**, 591–564.

Lanson, B. (1997) Decomposition of experimental X-ray diffraction patterns (profile fitting): a convenient way to study clay minerals. *Clays and Clay Minerals*, **45**, 132–146.

Linares, J. (1985) The process of bentonite formation in Cabo de Gata, Almería, Spain. *Mineralogica y Petrographica Acta*, **29-A**, 17–33.

Maury, R.C., Fourcade, S., Coulon, C., El Azzouzi, M., Bellon, H., Coutelle, A., Ouabadi, A., Semroud, B., Megartsi, M., Cotten, J., Belanteur, O., Louni-Hacini, A., Pique, A., Cardevila, R., Hernandez, J. and Rehault, J.P. (2000) Post-collisional neogene magmatism of the Mediterranean Maghreb margin: a consequence of slab break off. *Comptes Rendus de l'Académie des Sciences, Paris*, **331**, 159–173.

Meunier, A. and Velde, B. (1989) Solid solutions in I/S mixed layer minerals and illite. *American Mineralogist*, **74**, 1106–1112.

Meunier, A., Lanson, B. and Velde, B. (2004) Composition variation of illite-vermiculite-smectite mixed-layer minerals in a bentonite bed from Charente (France). *Clay Minerals*, **39**, 317–332.

Moore, D.M. and Reynolds, R.C. (1989) *X-ray Diffraction and the Identification and Analysis of Clay Minerals*. Oxford University Press, Oxford, UK.

Patrier, P., Beaufort, D., Mas, A. and Traineau, H. (2003) Surficial clay assemblage associated with the hydrothermal activity of Bouillante (Guadeloupe, French West Indies). *Journal of Volcanology and Geothermal Research*, **126**, 143–156.

Pique, A., Ait Brahim, L., El Azzouzi, M., Maury, R.C., Bellon, H., Semroud, B. and Laville, E. (1998) Le poinçon maghrébin : contraintes tectoniques et géochimiques. *Comptes Rendus de l'Académie des Sciences, Paris*, **326**, 575–581.

Plançon, A. and Drits, V.A. (2000) Phase analysis of clays using an expert system and calculation programs for X-ray diffraction by two- or three-component mixed-layer minerals. *Clays and Clay Minerals*, **48**, 57–62.

Reynolds, R.C. (1992) X-ray diffraction studies of illite/smectite from rocks, <1 μm randomly oriental powders, and <1 μm oriented powder aggregates. The absence of laboratory-induced artifacts. *Clays and Clay Minerals*, **40**, 387–396.

Sato, T., Watanabe, T. and Otsuka, R. (1992) Effects of layer charge, charge location, and energy change on expansion properties of dioctahedral smectites. *Clays and Clay Minerals*, **40**, 103–113.

Senkayi, A.L., Dixon, J.B., Hossner, L.R., Abder-Ruhman, M. and Fanning, D.S. (1984) Mineralogy and genetic relationships of tonstein, bentonite, and lignitic strata in the Eocene Yegua formation of East-Central Texas. *Clays and Clay minerals*, **32**, 259–271.

Weaver, C.E (1989) *Clay, Muds and Shales*. Developments in Sedimentology, **44**. Elsevier, Amsterdam, 819 pp.

Yamada, H., Yoshioka, K., Tamura, K., Fujii, K. and Nakazawa, H. (1999) Compositional gap in dioctahedral-trioctahedral smectite system: beidellite-saponite pseudo-binary join. *Clays and Clay Minerals*, **47**, 803–810.

Zielinski, R.A. (1979) Uranium mobility during interaction of rhyolitic obsidian, perlite and felsite with alkaline carbonate solution: T=120ºC, P=210 kg/cm^2. *Chemical Geology*, **27**, 47–63.

Zielinski, R.A. (1980) Stability of glass in the geologic environment: some evidence from studies of natural silicate glasses. *Nuclear Technology*, **51**, 197–200.

Zielinski, R.A. (1982) The mobility of uranium and other elements during alteration of rhyolite ash to montmorillonite : A case study in the Troublesome formation, Colorado, USA. *Chemical Geology*, **35**, 185–204.

Zielinski, R.A. (1985) Element mobility during alteration of silicic ash to kaolinite – a study of tonstein. *Sedimentology*, **32**, 567–579.

(*Received 4 August 2004; revised 17 January 2005; Ms. 948; A.E. W. Crawford Elliott*)